

Miscibility and Thermal and Crystallization Behaviors of Poly(D-(–)-3-hydroxybutyrate)/Atactic Poly(methyl methacrylate) Blends

A. Siciliano, A. Seves, and T. De Marco

Stazione Sperimentale per la Cellulosa, Carta e Fibre Tessili Vegetali ed Artificiali,
Piazza L. da Vinci 26, 20133 Milano, Italy

S. Cimmino,* E. Martuscelli, and C. Silvestre

Istituto di Ricerca e Tecnologia delle Materie Plastiche, Via Toiano 6,
80072 Arco Felice (NA), Italy

Received February 28, 1995*

ABSTRACT: The miscibility of poly(D-(–)-3-hydroxybutyrate)/atactic poly(methyl methacrylate) (PHB/aPMMA) blends has been investigated as a function of blend composition and thermal treatments. The DSC thermograms obtained by heating up samples of PHB/aPMMA blends quenched from 200 and from 185 °C to liquid nitrogen temperature show the presence of a single glass transition temperature, whereas the thermograms of blends annealed at temperatures selected in the range 140–170 °C display the presence of two glass transition temperatures. The SEM analysis of the fractured surfaces of the samples show that the quenched blends are homogeneous, whereas two phases are present in the annealed blends. The results have been accounted for by assuming an upper critical solution temperature (ucst). At $T > \text{ucst}$, the PHB and aPMMA components are completely miscible at all compositions, whereas at lower temperature the melt phase separates in the two pure components. The glass transition behavior observed for the quenched blends has been interpreted by using the free volume theory presented by Kovacs. This theory has been shown to describe the experimental T_g values as a function of blend composition if the interaction term g is assumed negative.

Introduction

Poly(D-(–)-3-hydroxybutyrate) (PHB) is a natural aliphatic polyester produced by bacterial fermentation. PHB has attracted much interest for medical and agricultural applications because it is biodegradable and highly biocompatible. The use of PHB has some limitations: high cost production, a very narrow processability window, and a relatively low impact resistance. In fact PHB degrades to crotonic acid if it is kept at a temperature of only few degrees above its melting point for a relatively long time; the injection-molded samples have a high crystallinity degree and show brittle behavior, especially at temperatures below the glass transition temperature (T_g).

In order to improve the physical properties of PHB it has been attempted to blend a second polymer component. In literature are reported studies of blends of PHB with poly(ethylene oxide)¹ (PEO), poly(vinyl acetate)² (PVAc), poly(epichlorohydrin),^{3,4} cellulose esters,⁵ and aPMMA.^{6,7}

In ref 8 the phase structure of PHB/aPMMA 100/0, 70/30, 60/40, and 50/50 wt % blends, isothermally crystallized from low T , was investigated. The samples were melted at 185 °C for 1 min and then quenched in an ice–water mixture and finally crystallized isothermally. It was found that the crystalline lamellae and the transition layer thicknesses are independent of composition, whereas the average long period thickness increases with the aPMMA content in the samples, indicating that the all-aPMMA component is segregated in the interlamellar regions during the isothermal crystallization; these results indicate that the two components are miscible in the amorphous state at 185

°C. The PHB/aPMMA system has been also investigated by Lotti et al.⁷ These investigators explained their results by assuming that the two components form a glass amorphous single phase with compositions up to 20 wt % of PHB; at concentration of PHB higher than 20 wt %, the blends are formed by plain PHB coexisting with a constant composition PHB/aPMMA 20/80 wt % blend. The present paper reports an investigation on the morphological analysis and thermal properties of PHB/aPMMA blends.

The aim of this work is to investigate further the miscibility of the PHB/aPMMA blends in the melt in order to define if the two components are completely or partially miscible or confirm the miscibility limit of PHB in the blends, as reported in ref 7.

Experimental Section

Materials. The polymers used are PHB (ICI), $M_w = 1.59 \times 10^5$ and $M_w/M_n = 3.2$ and aPMMA (BDH), $M_w = 1.16 \times 10^5$ and $M_w/M_n = 3$.

Blend Preparation. PHB/aPMMA blends with weight ratios from 100/0 to 0/100 were prepared by solution casting from chloroform and, after the precipitation, kept in vacuum oven at 70 °C for 8 h.

Calorimetric Measurements. Differential scanning calorimeter (Perkin-Elmer, DSC-4) was used to determine the thermal properties of the blends. Each sample (about 15 mg), after the thermal program reported below, was scanned from –50 to 200 °C at heating rate 20 °C/min. From the thermograms one or two glass transitions were detected depending on whether or not phase separation had taken place during the thermal treatments.

The T_g value was taken as the temperature corresponding to the maximum of the peak of the first-order derivative of the transition trace. The temperature of the cold crystallization peak, T_c , and the melting temperature, T_m , were taken as the temperature corresponding to the maximum of the exothermic and endothermic peak respectively.

* To whom correspondence should be addressed.

† Abstract published in *Advance ACS Abstracts*, October 1, 1995.

Three main thermal programs were used to influence the miscibility of the blends, labeled as *quenching*, *cooling*, and *annealing programs*.

Times and temperatures were chosen with care in order to limit the thermal degradation of PHB according to results obtained by Grassie et al.⁸

(a) Quenching Program. Two melting temperatures were used, 185 and 200 °C. The melting times were 10 s at 200 °C and 1 min at 185 °C. The sample was set in a DSC pan and melted in the oven of the DSC. After the melting time elapsed, the sample was immediately transferred in a Dewar vessel with liquid nitrogen and kept there for several minutes. The time for transferring the sample from the oven into liquid nitrogen was less than 2 s. The Dewar vessel was inside the drybox of the DSC-4. After the quenching, the sample was set again in the DSC oven whose temperature was at -50 °C for the scanning. This sample is named through the work as quenched blend and coded as 200-q-blend and 185-q-blend, where the number stands for the melting temperature and the letter q for "quenched".

(b) Cooling Program. The sample was melt at 200 °C for 10 s and then cooled at -50 °C setting the cooling rate of the DSC at the maximum value, 320 °C/min. This sample is named through the work as cooled blend.

(c) Annealing Program. The sample was melt at 200 °C for 10 s and annealed at selected temperature for 5 min; the sample was then quenched in liquid nitrogen for several minutes and finally set at -50 °C in the DSC; the selected temperatures for the annealing were 170, 155, and 140 °C; temperatures lower than 140 °C were not used because the PHB crystallizes isothermally; the annealing treatment at 140 °C was also performed for 40 min. The sample of the annealing program is named through the work as annealed blend.

The comparison of the values of the enthalpy of fusion (ΔH_f) and enthalpy of crystallization peak (ΔH_{cc}) of the pure PHB and 90/10 to 60/40 PHB/aPMMA (quenched, cooled, or isothermally heated) blends has shown that the two values are equivalent, indicating that these blends are at the beginning of the DSC scanning (-50 °C) amorphous. The comparison of the ΔH_f and ΔH_{cc} for the blends with higher aPMMA content is not possible because the determination of the ΔH_{cc} depends very much on the method of integration used. Our interpretation is that the presence of aPMMA molecules in the 50/50 to 10/90 PHB/aPMMA blends slows down the crystallization process, and for these blends the crystallization peaks do not represent all of the amount of the crystallization that still remains at temperatures higher than the peaks. Considering that the pure PHB and the blends with a high content of PHB are found to be amorphous and that these are the blends more difficult to obtain in the amorphous state by quenching or cooling processes from the melt, it is reasonable to conclude that the 50/50 to 10/90 blends are also amorphous at the beginning of the DSC scanning. The aPMMA molecules in this system can only disturb and slow down the crystallization.

Scanning Electron Microscopy. The analysis of the phase morphology was investigated by scanning electron microscopy (SEM). The samples investigated were the 200-q-blends, the 185-q-blends and the annealed blends at 140 °C for 40 min. Each sample was bathed in liquid nitrogen for at least 5 min and then soon split. The surfaces obtained by the splitting were coated by Au evaporation and examined by a Philips 515 scanning electron microscope.

Results and Discussion

Glass Transition Temperature. Figure 1 reports the normalized thermograms of the 200-q-blends. The thermograms of the 185-q-blends are not shown because they are identical to the 200-q-blends at a parity of composition.

The thermograms of plain PHB and aPMMA quenched samples show the T_g at 5 ± 2 and 119 ± 2 °C respectively. All the thermograms of the quenched blends present a unique glass transition temperature. In particular, the thermograms of the 90/10 and 80/20

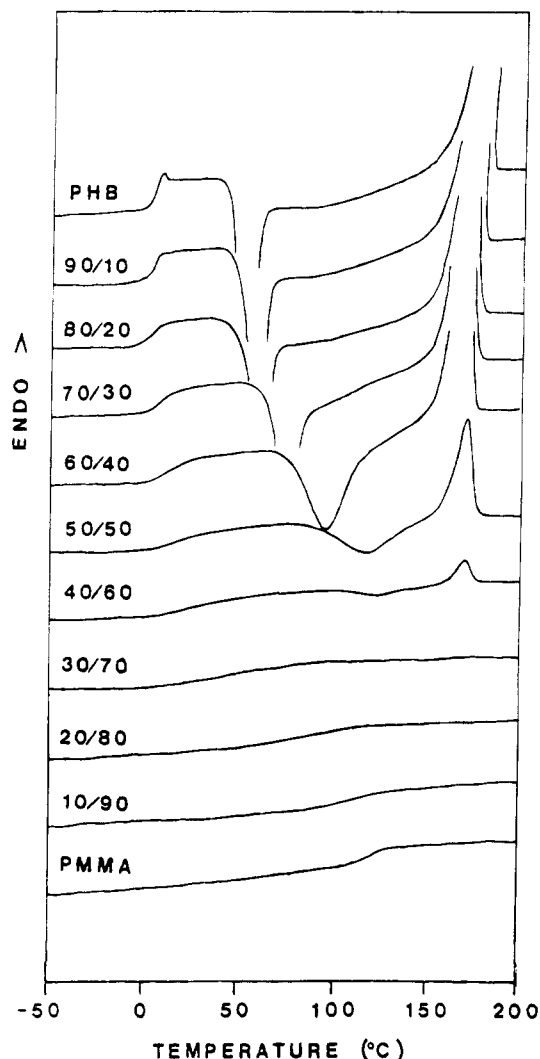


Figure 1. Normalized DSC thermograms of PHB/aPMMA quenched blends.

quenched blends present the T_g at same value of the glass transition temperature of plain PHB and no other transition in the range of the T_g of aPMMA. The T_g s of the quenched blends with compositions from 70/30 to 10/90 increase with the aPMMA content in the mixture.

Figure 2 reports the normalized thermograms of the cooled blends. The blends with composition from 90/10 to 30/70 PHB/aPMMA present two glass transition temperatures constant with composition. The first transition is at about 5 ± 2 °C and the second at about 119 ± 2 °C, that is, the same values of the plain homopolymers. The 20/80 and 10/90 PHB/aPMMA cooled blends, instead, show only one glass transition temperature, whose value depends on the composition and is the same as the T_g s of the corresponding blends of Figure 1.

Figures 3 and 4 show the thermograms of the 90/10 to 30/70 PHB/aPMMA blends annealed for 5 min at 140 and 170 °C, respectively. For the sake of clarity the thermograms of the blends annealed at 155 °C and those of the blends annealed at 140 for 40 min are not presented: they are similar to those reported in Figures 3 and 4.

From the analysis of the thermograms of Figure 3 it is observed that the annealed PHB/aPMMA samples from composition 90/10 to 40/60 present two distinct and constant glass transition temperatures. The first T_g is at about 5 °C and the second one in the range 115–120 °C. The thermogram of the 30/70 quenched blend also

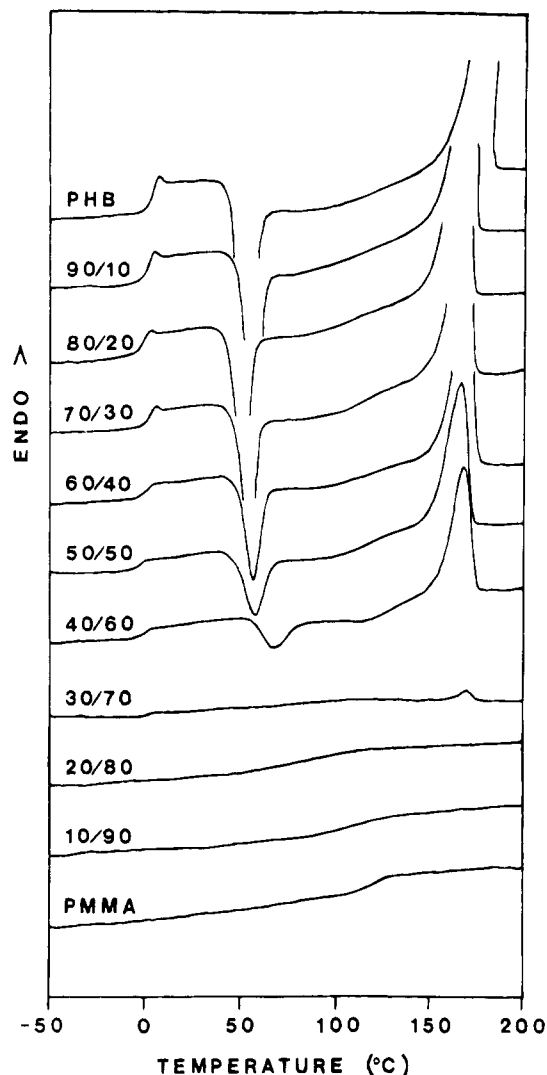


Figure 2. Normalized DSC thermograms of PHB/aPMMA cooled blends.

shows the T_g at about 5 °C, but the second T_g is not detectable. This is very likely due to the nearness of the cold crystallization peak. In fact the cold crystallization peak of annealed blends with high aPMMA content, moves toward at higher T with the consequence that it alters the step of the second T_g . The same general behavior is observed in Figure 4 relative to the blends annealed at 170 °C, and in this case the blends that show the two T_g s are those with compositions from 90/10 to 50/50.

The 20/80 and 10/90 PHB/aPMMA annealed blends present a very interesting behavior of the glass transition temperatures. Figure 5 reports, as an example, the thermograms of the 20/80 and 10/90 blends annealed at 140 °C for 40 min (curve a), and 155 and 170 °C for 5 min (curves b and c respectively). The thermograms of the 20/80 and 10/90 blends annealed at 170 °C (curve c in Figure 5) present one glass transition temperature, whose values are the same of the T_g of the corresponding quenched blends, whereas the thermograms of the blends annealed at temperatures lower than 170 °C show two distinct glass transition temperatures.

The T_g behaviors of the quenched, cooled, and annealed blends can be accounted for by assuming that the PHB and aPMMA homopolymers form one miscible phase at 200 and 185 °C for all composition and that an upper critical solution temperature (ucst) is in the temperature range 170–185 °C for the 90/10 to 30/70

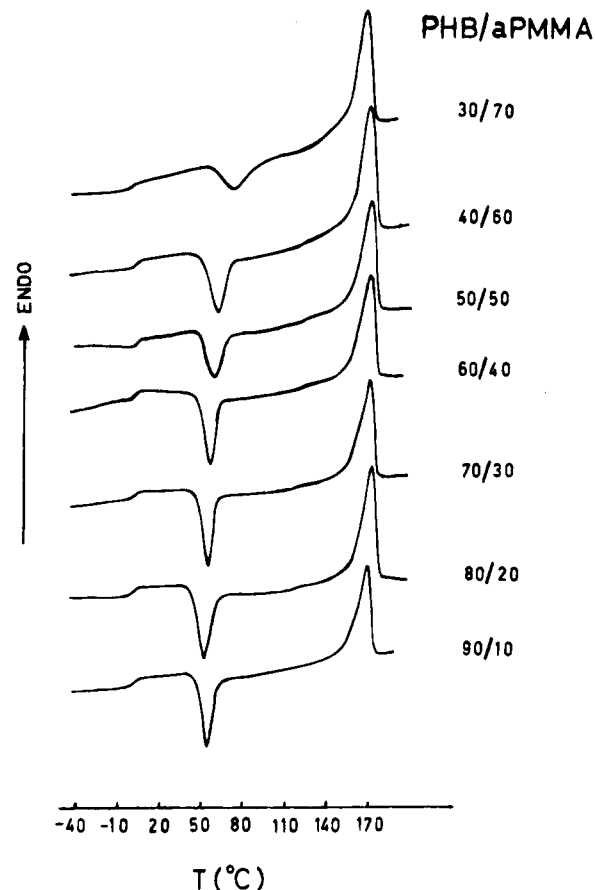


Figure 3. Normalized DSC thermograms of PHB/aPMMA blends annealed at 140 °C for 5 min before sudden quenching in liquid nitrogen.

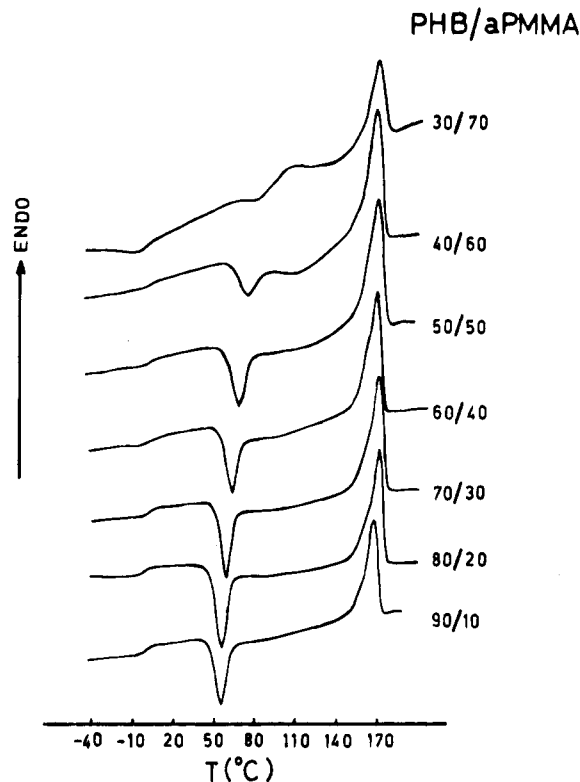


Figure 4. Normalized DSC thermograms of PHB/aPMMA blends annealed at 170 °C for 5 min before sudden quenching in liquid nitrogen.

blends and in the range 155–170 °C for the 20/80 and 10/90 blends. This hypothesis is sketched in the upper part of Figure 6 where the open circles represents the

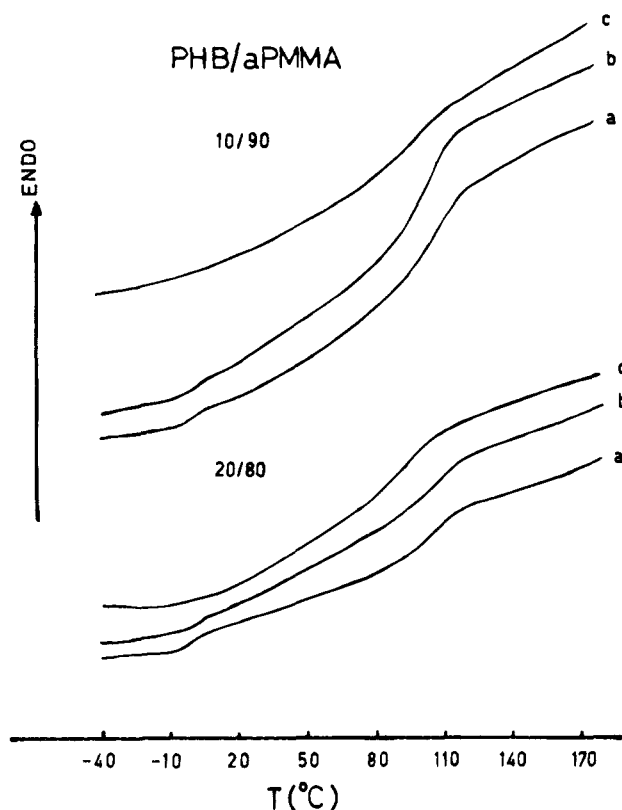


Figure 5. Normalized DSC thermograms of 20/80 and 10/90 PHB/aPMMA annealed blends: (a) sample annealed at 140 °C for 40 min; (b) sample annealed at 155 °C for 5 min; and (c) sample annealed at 170 °C for 5 min.

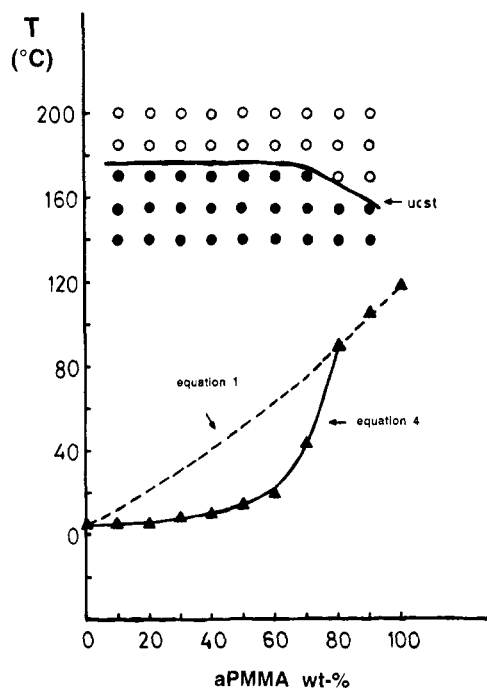


Figure 6. Phase diagram of PHB/aPMMA blends: (○) one phase; (●) two phases; (▲) experimental glass transition temperatures of quenched blends.

miscible state and the filled circles the phase separation state of the PHB/aPMMA system. The line drawn among the circle represents roughly the ucst curve. Moreover the T_g s of the quenched blends are reported in the same figure (filled triangles). Figure 6 can be considered as a pseudo phase diagram of the amorphous state of the PHB/aPMMA system; the figure does not

contain any reference to the crystallization phenomenon.

When the homogeneous phase, of any composition, is quenched instantly from 200 or 185 °C into liquid nitrogen, the quenching process is very fast to avoid phase separation. The solidified sample conserves the structure that it had in the melt and the relative thermogram shows one glass transition; see Figure 1. So the T_g s of the quenched blends represent the T_g s of the miscible blends.

When the 90/10 to 30/70 PHB/aPMMA blends, after melting, are annealed at 170, 155, and 140 °C, the homogeneous melt phase separates in two phases, and the relative thermograms present two glass transition temperatures; see Figures 3 and 4.

The 20/80 and 10/90 blends would have the critical solution temperatures in the range 170–155 °C. In fact the 20/80 and 10/90 blends annealed at 170 °C present thermograms with one glass transition, whereas for blends annealed at 155 and 140 °C two clear T_g s are observed (see Figure 5).

The phase diagram proposed in Figure 6 would explain also the behaviors of the cooled blends; i.e. the 90/10 to 30/70 cooled blends result in separated phases, whereas the 20/80 and 10/90 cooled blends result in a miscible phase. The glass transition temperatures relative to the homogeneous melt phase of 90/10 to 30/70 PHB/aPMMA blends are at about 160–130 deg lower than the ucst curve, depending on composition. The melt of these blends, cooled at maximum rate of DSC, takes about 20–30 s to reach temperatures lower than T_g where the homogeneous phase would be frozen; this time seems enough to allow the phase separation. For the 20/80 and 10/90 blends, not only are the critical solution temperatures lower but the T_g s of the homogeneous phase have much higher values, about 90 and 105 °C, respectively (see Figure 6). So the melt of these two blends goes through a smaller two-phase region and reaches $T < T_g$ in a few seconds and the phase separation does not take place.

It could be argued that the PHB/aPMMA blends result in a miscible phase at 200 and 185 °C because the times of melting, 10 s and 1 min, respectively, were not sufficient to generate the phase separation of the components. Since higher times of melting were not possible because of the degradation of PHB,⁸ some experiments were also performed at 170, 155, and 140 °C with annealing times of 10 and 30 s. The thermograms of these blends were similar to those presented in Figures 3 and 4. Moreover, blends annealed at 140 °C for 40 min (found not miscible as shown in Figure 4) have been again melted at 200 °C for 10 s and at 185 °C for 1 min and finally quenched in liquid nitrogen. The final thermograms were identical to those of quenched blends shown in Figure 1, that is, the blends returned again to miscible. These experiments indicate that the conversions from the two-phase region to one-phase region and vice versa are reversible and fast.

Morphology. The existence of the upper critical solution temperature curve for PHB/aPMMA system was confirmed by the SEM analysis.

Figures 7 and 8 show, as an example, the fractured surfaces of the 60/40 and 40/60 PHB/aPMMA quenched blends and annealed blends at 140 °C for 40 min, respectively. It is found that the fractured surfaces of the quenched blends are homogeneous and smooth, whereas the surfaces of the annealed samples are not homogeneous, with the presence of two phases that seem to be very interconnected. The morphology found for the 200-q-blends (see Figures 7a and 8a) derives

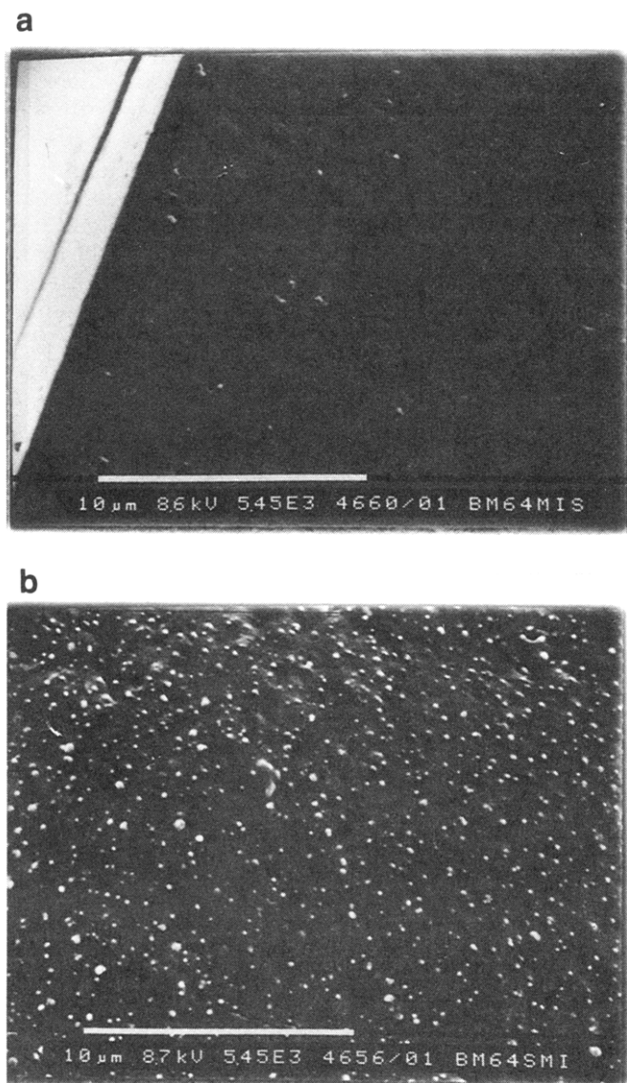


Figure 7. SEM micrographs of 60/40 PHB/aPMMA blend: (a) 200-q-blend and (b) annealed at 140 °C for 40 min.

from the fact that the two components are miscible at 200 °C, whereas the morphologies of the annealed blends (see Figures 7b and 8b) clearly indicate that the system is phase separated.

Cold Crystallization Peak. The cold crystallization process of PHB/aPMMA blends is dependent on the thermal treatment. In particular, the cold crystallization peak of the quenched blends, see Figure 1, moves toward higher temperatures with the aPMMA content, whereas the temperatures of the cold crystallization peaks of cooled and annealed blends (see Figures 2–4) are almost constant (or increase slightly) up to the composition 50/50 and then the increase is more decided for blends with higher aPMMA content. No cold crystallization peak is present for the 20/80 and 10/90 PHB/aPMMA cooled and annealed blends.

The increase of the cold crystallization peak temperature observed for the quenched blends from the composition 90/10 to 40/60, see Figure 9, can be explained considering that the crystallization process takes place from a single homogeneous phase. The viscosity of this phase increases with aPMMA content. Moreover the presence of aPMMA causes a dilution of the PHB nuclei. Both of these effects would determine a decrease in the overall crystallization rate, and so the increase of the cold crystallization peak. The energy term relative to the formation of a nucleus of critical size, very predominant in the case of crystallization process close to T_m ,

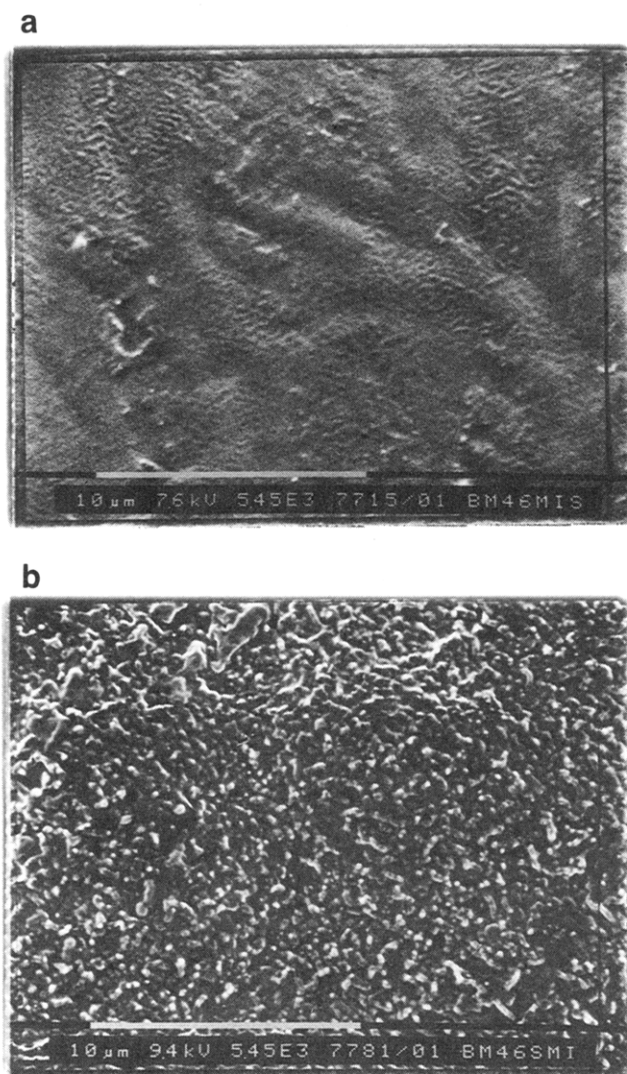


Figure 8. SEM micrographs of 40/60 PHB/aPMMA blend: (a) 200-q-blend and (b) annealed at 140 °C for 40 min.

is very likely not important in this case where the crystallization occurs from the cold.

Different is the case for the cooled and annealed blends. For these blends the crystallization process takes place in presence of two phases, the PHB phase and the aPMMA phase, which are completely interconnected, as the analysis of the SEM micrographs show; see Figures 7b and 8b. In the case of not miscible blends, the presence of a noncrystallizable material can influence only the transport term. Since the PHB component crystallizes from its own phase, up to the composition 50/50 the crystallization does not suffer from the presence of the aPMMA phase and the cold crystallization peak is present more or less at the same temperature. At higher aPMMA content, the crystallization of PHB is influenced by the higher number and bigger aPMMA domains that probably must be rejected from the crystallization front. The energy required for the rejection would induce the delay of the crystallization process with the consequence that the cold crystallization peak moves at higher temperatures.

Melting Temperature. It is important to consider that the T_m s in examination are not equilibrium points and not relative to samples crystallized isothermally, but they were obtained from samples that crystallized from cold during the scanning in the DSC.

The observed melting temperature values of the quenched blends as a function of composition are

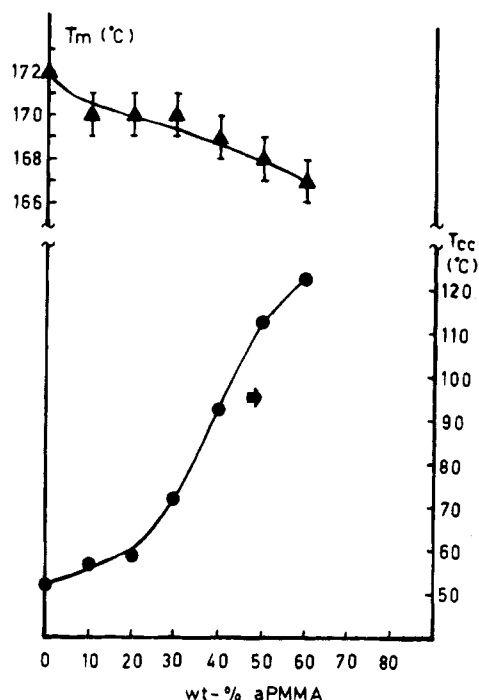


Figure 9. Experimental melting point and cold crystallization peak temperature of PHB/aPMMA quenched blends as a function of blend composition.

reported in Figure 9. It is observed that the T_m decreases with the aPMMA content: in fact the T_m of pure quenched PHB sample is 172 °C and that of 40/60 PHB/aPMMA quenched blend is 167 °C. Different is the trend of T_m of the annealed blends: a T_m value of 172 ± 2 °C is always obtained.

In general the melting point of blends depends on both morphological and thermodynamic factors. The morphological factors are related to crystallization temperature, crystallization time, blend composition, and scanning rate: some of these factors can cause increase and/or decrease of T_m . They are the only factors that can influence the T_m in the case of not miscible blends. In the case of miscible blends also the thermodynamic factor must be considered, whose contribution can only induce the decrease of T_m .

The decrease of T_m of the quenched blends increasing aPMMA content (see Figure 9) is very likely the result of several effects: depression of the equilibrium melting point, since the two components are miscible in the quenched blends; decrease of the annealing process that occurs during the scanning of the samples, whose effect decreases as the cold crystallization peak approaches remarkably T_m ; and formation of less perfect crystals increasing aPMMA content in the blend. All these factors outweigh evidently the contrary effect that is derived from the remarkable increase of the cold crystallization peak. In fact the increase of the cold crystallization peak should cause the formation of crystals at higher temperatures, i.e. with higher lamellar thickness and hence higher T_m .

The constancy of T_m of the annealed blends, 172 ± 2 °C, is consistent with the phase diagram of Figure 6. The annealing processes, carried out at temperatures between 140 °C and the ucsd curve, produce the demixing of the blends in two phases: PHB phase and aPMMA phase. So the PHB crystallizes from its own phase, forming crystals during the cold crystallization, which melt at constant T independent of composition and crystallization temperature.

T_g Analysis of Quenched Blends. In this section the trend of the glass transition temperatures of the quenched (miscible) blends is analyzed. The values of the T_g s are reported in Figure 6, together with the curves derived by Fox's and Kovacs's theories.

The examination of the T_g data in Figure 6 indicates that the T_g of the blend with aPMMA content up to 40 % wt, is almost constant; at higher aPMMA content, the T_g increases remarkably. The general trend of the data shows the presence of a break or cusp at composition between 30/70 and 20/80 PHB/aPMMA and temperature range 50–90 °C.

There are several equations, derived from the free volume hypothesis or from thermodynamic arguments, proposed to predict the T_g -composition dependence of miscible blends, as those prompted by Couchman-Karas, Gordon-Taylor,¹⁰ Utracki,¹¹ and Fox.¹² These equations, with different approximations, predict a monotonic dependence of T_g upon composition, and do not give any cusp in the predicted curve.

As an example, the curve obtained by the most used expression of T_g -composition dependence of miscible polymer blends, the Fox equation,¹² is reported in Figure 6:

$$\frac{1}{T_g} = \frac{W_1}{T_{g1}} + \frac{W_2}{T_{g2}} \quad (1)$$

where T_g is the glass transition temperature of the blend, W_i and T_{gi} are the weight fraction and the glass transition temperature of the component i respectively.

Equation 1 assumes random mixing between the components, equality of the differences in specific heat between the liquid, and the glassy states at T_{gi} of the components (i.e. $\Delta C_{p1} = \Delta C_{p2}$), and no excess volume between the two components upon mixing.

The predicted curve of Fox equation is obtained by setting $T_g(\text{PHB}) = 278$ K and $T_g(\text{aPMMA}) = 392$ K. It is observed that only the T_g of the 10/90 and 20/80 PHB/aPMMA blends are fitted by the Fox equation and all the other experimental T_g s lie much below the predicted curve. The result is the same if the equations proposed by Couchman-Karas, Gordon-Taylor, and Utracki are used: the predicted curves fit satisfactorily only the T_g s of the 20/80 and 10/90 PHB/aPMMA blends.

Trends of T_g of miscible blends with a cusp on T_g -composition curve have been already reported by Roy et al.,¹³ Nandi et al.,¹⁴ and Prud'homme et al.¹⁵

There are two theoretical treatments able to describe the peculiar T_g -composition trends with the cusp: that proposed by Righetti et al.^{16–18} and the Kovacs theory.^{19,20} Righetti et al.^{16–18} have shown that the Couchman treatment is able to describe the experimental data of a system which exhibits a cusp in the T_g -composition curve if the temperature dependence of the specific heat increments is considered and the characteristic temperature, T_0 , is computed. We have preferred in this work to use the Kovacs theory that was shown by Aubin et al.¹⁵ to describe well the peculiar trend with the cusp. Kovacs,^{19,20} in the framework of the free volume theory, has shown that if the difference of the T_g s between the two homopolymers ($T_{g2} - T_{g1}$) is larger than 50 deg, there is a temperature defined as the critical temperature (T_c) where the free volume of polymer with higher glass transition temperature (T_{g2}) becomes zero. The critical temperature and the corresponding critical volume fraction ϕ_c (relative to the polymer with lower T_g), calculated by Kovacs are

$$T_c = T_{g2} - (f_{g2}/\Delta\alpha_2) \quad (2)$$

$$\phi_c = f_{g2}/[\Delta\alpha_1(T_{g2} - T_{g1}) + f_{g2}(1 - \Delta\alpha_1/\Delta\alpha_2)] \quad (3)$$

where $T_{g2} > T_{g1}$; f_{gi} is the free volume fraction of polymer i , and $\Delta\alpha_i$ the difference between the volume expansion coefficients in the glassy and liquid states.

Kovacs has shown that below T_c the T_g of the blend is given by

$$T_g = T_{g1} + \frac{\phi_2 f_{g2} + g \phi_1 \phi_2}{\phi_1 \Delta\alpha_1} \quad (4)$$

where ϕ_i is the volume fraction and g is an interaction term defined by

$$g = V_e/V\phi_1\phi_2 \quad (5)$$

where V is the volume of the blend and V_e the excess volume.

The term g is equal to zero if there is no excess volume between the two polymers upon mixing ($V_e = 0$); g is positive if the interactions between the two components in the blends are stronger than the average interactions between molecules of the same species, and it is negative if the average interactions between blend components are weaker than those between molecules of the same species.

The calculated values of T_c (eq 2) and ϕ_c (eq 3) for PHB/aPMMA system are found to be 79 °C and 0.31 respectively, and they mean that for $T < 79$ °C and for compositions from 90/10 to 30/70 PHB/aPMMA, the expressions of Couchman–Karasz, Gordon–Taylor, Utracki, and Fox are not valid, but they can be used only for temperatures and composition higher than the critical ones. The critical values were calculated by using the following parameters: $T_{g1} = 278$ K and $T_{g2} = 392$ K (experimental data); $f_{g2} = 0.013$ (from refs 21 and 22); $\Delta\alpha_1 = 4.0 \times 10^{-4}$ K⁻¹ (from ref 23; $\Delta\alpha_1$ is computed assuming the validity of Simha–Boyer rule $\Delta\alpha_1 T_{g1} = 0.015$); and $\Delta\alpha_2 = 3.2 \times 10^{-4}$ K⁻¹ (from ref 24); eq 4 was used to fit the T_g s of PHB/aPMMA blends from composition 90/10 to 30/70; and ϕ_1 and ϕ_2 were calculated by setting the density of PHB = 1.15 g/cm³,²⁵ and the density of aPMMA = 1.118 g/cm³.²⁴

The Kovacs equation fits the data setting the parameter $g = -0.018$ (solid line in Figure 6). The negative value of g means that the average interactions between blend components are weaker than those between molecules of the same species, i.e. no specific interactions should exist.

This point and the presence of the ucst require a comment. The ucst behavior is generally observed in polymer–solvent and polymer–oligomer systems and it is rather uncommon in polymer–polymer blends. Nevertheless there are several examples of ucst behavior for polymer blends reported in literature like those of Karasz^{26,27} and Inoue.^{28–30} Theoretically the ucst behavior can be predicted both by the Flory–Huggins theory and the Prigogine–Flory equation of state theory. In the Flory–Huggins theory, for a system where there are no specific interactions, the ucst behavior derives from the decrease of the Gibbs free energy of mixing with increasing the temperature. McMaster,³¹ in the framework of the Prigogine–Flory equation of state theory, demonstrated that a polymer–polymer system with a small positive exchange interactional energy term and a very small free volume contribution can exhibit both ucst and lower critical solution temperature

(lcst) and this could be the case of PHB/aPMMA system. Of course the existence of the lcst behavior cannot be experimentally verified because it is very likely located at high temperatures (higher than 200 °C) where the PHB undergoes remarkable thermal degradation.

Finally we compare the results reported by Lotti et al.⁷ to those of cooled blends, because the thermal treatment performed in ref 7 is similar to our cooling program. Only the 20/80 and 10/90 blends are reported as miscible and this is in agreement with our results because the quenching used in ref 7 is sufficient to freeze only these two blends from the miscible region to temperatures lower than the T_g s (see Figure 6). But no annealing was performed on these two blends at $T < 170$ °C.

The blends with PHB concentration exceeding 20 wt % are reported in ref 7 to be formed by a pure PHB phase coexisting with a constant-composition 20/80 PHB/aPMMA blend. We also have found that these blends are phase separated, but only at $T \leq 170$ °C and in the pure components. These dissimilarities could be due to the different blend preparation used in ref 7: the blends were prepared by mixing the components at 195 °C for 3 min, then injection-molded, and finally quenched in an ice–water mixture. This procedure could have produced thermal degradation of PHB, as reported by Grassie et al.,⁸ with the formation of a low molecular weight fraction that would result in more miscibility with the aPMMA component, whose molecular weight is not reported.

Conclusions

The PHB/aPMMA blends are shown to present an ucst behavior. The miscibility can be detected only with a quasiinstantaneous quenching (quenching program) from the one-phase region to temperatures lower than T_g . The fastest cooling rate of the DSC is sufficient to conserve the homogeneous melt phase only for the 20/80 and 10/90 PHB/aPMMA blends. The two-phase region has been detected by annealing the blends at selected temperatures in the melt followed by a rapid quenching in liquid nitrogen. The glass transition temperatures of the miscible blends present a trend with a cusp and only the T_g of the 10/90 and 20/80 PHB/aPMMA blends follow the prediction of the Fox equation. The T_g of the other blends lie much below the predicted curve. This peculiar trend has been accounted for by the Kovacs theory. It is shown that the Kovacs equation describes the T_g trends of the 90/10 to 30/70 PHB/aPMMA blends if the interaction parameter of the theory is assumed negative, i.e. the average interactions between blend components are weaker than those between molecules of the same species.

Acknowledgment. The authors warmly thank Mrs. V. Richter for the SEM experiments.

References and Notes

- (1) Avella, M.; Martuscelli, E. *Polymer* **1988**, *29*, 1731.
- (2) Greco, P.; Martuscelli, E. *Polymer* **1989**, *30*, 1475.
- (3) Dubini Paglia, E.; Beltrame, P. L.; Canetti, M.; Seves, A.; Mercandalli, B.; Martuscelli, E. *Polymer* **1993**, *34*, 996.
- (4) Sadocco, P.; Canetti, M.; Seves, A.; Martuscelli, E. *Polymer* **1993**, *34*, 3369.
- (5) Scandola, M.; Ceccorulli, G.; Pizzoli, M. *Macromolecules* **1992**, *25*, 6441.
- (6) Canetti, M.; Sadocco, P.; Siciliano, A.; Seves, A. *Polymer* **1994**, *35*, 2884.
- (7) Lotti, N.; Pizzoli, M.; Ceccorulli, G.; Scandola, M. *Polymer* **1993**, *34*, 35.

- (8) Grassie, N.; Murray, E. J.; Holmes, P. A. *Polym. Degrad. Stab.* **1984**, *6*, 95.
- (9) Couchman, P. R.; Karasz, F. E. *Macromolecules* **1978**, *11*, 117.
- (10) Gordon, M.; Taylor, J. S. *J. Appl. Chem.* **1952**, *2*, 493.
- (11) Utracki, L. A. *Adv. Polym. Technol.* **1985**, *5*, 33.
- (12) Fox, T. G. *Bull. Am. Phys. Soc.* **1956**, *2*, 123.
- (13) Roy, S. K.; Brown, G. R.; St-Pierre, L. E. *Int. J. Polym. Mater.* **1983**, *10*, 13.
- (14) Nandi, A. K.; Mandal, B. M.; Bhattacharyya, S. N.; Roy, S. K. *Polym. Commun.* **1986**, *27*, 151.
- (15) Aubin, M.; Prud'homme, R. E. *Macromolecules* **1988**, *21*, 2945.
- (16) Righetti, M. C.; Ajroldi, G.; Pezzin, G. *Polymer* **1992**, *33*, 4779.
- (17) Righetti, M. C.; Ajroldi, G.; Pezzin, G. *Polymer* **1992**, *33*, 4786.
- (18) Righetti, M. C.; Ajroldi, G.; Marchionni, G.; Pezzin, G. *Polymer* **1993**, *34*, 4307.
- (19) Kovacs, A. J. *Adv. Polym. Sci.* **1963**, *3*, 394.
- (20) Braun, G.; Kovacs, A. J. In *Physics of noncrystalline solids*; Prins, J. A., Ed.; North-Holland: Amsterdam, 1965.
- (21) O'Connor, K. M.; Scholsky, K. M. *Polymer* **1989**, *30*, 461.
- (22) Berry, G. C.; Fox, T. G. *Adv. Polym. Sci.* **1967**, *5*, 261.
- (23) van Krevelen, D. W. In *Properties of Polymers*; Elsevier: Amsterdam, The Netherlands, 1976; Chapter 4, p 68.
- (24) Wunderlich, W. Physical Constants of Poly(methyl methacrylate). In *Polymer Handbook*, 3rd ed.; Brandrup, J., Immergut, E. H., Eds.; J. Wiley and Sons: New York, 1989.
- (25) Bharam, P. J.; Keller, A.; Otun, E. L.; Holmes, P. A. *J. Mater. Sci.* **1984**, *19*, 2781.
- (26) Ueda, H.; Karasz, F. E. *Macromolecules* **1985**, *18*, 2719.
- (27) Cong, G.; Huang, Y.; McKnight, W. J.; Karasz, F. E. *Macromolecules* **1986**, *18*, 2765.
- (28) Ougizawa, T.; Inoue, T.; Kammer, H. W. *Macromolecules* **1985**, *18*, 2089.
- (29) Ougizawa, T.; Inoue, T. *Polym. J.* **1986**, *18*, 521.
- (30) Saito, H.; Fujita, Y.; Inoue, T. *Polym. J.* **1987**, *19*, 405.
- (31) McMaster, L. P. *Macromolecules* **1973**, *6*, 760.

MA950253Q